

# Numerical study of magnetic and pairing correlation in bilayer triangular lattice

Shuang Wu<sup>1</sup>, Jinling Li<sup>1</sup>, Pan Gao<sup>1</sup>, Ying Liang<sup>1</sup>, Tianxing Ma<sup>1,2,\*</sup>

<sup>1</sup>*Department of Physics, Beijing Normal University, Beijing 100875, China*

<sup>2</sup>*Beijing Computational Science Research Center, Beijing 100084, China*

(Dated: September 24, 2018)

By using the determinant Quantum Monte Carlo method, the magnetic and pairing correlation of the  $\text{Na}_x\text{CoO}_2 \cdot y\text{H}_2\text{O}$  system are studied within the Hubbard model on a bilayer triangular lattice. The temperature dependence of spin correlation function and pairing susceptibility with several kinds of symmetries at different electron fillings and inter layer coupling terms are investigated. It is found that the system shows an antiferromagnetic correlation around the half filling, and the  $fn$ -wave pairing correlation dominates over other kinds of pairing symmetry in the low doping region. As the electron filling decreases away from the half filling, both the ferromagnetic correlation and the  $f$ -wave pairing susceptibility are enhanced and tend to dominate. It is also shown that both the magnetic susceptibility and pairing susceptibility decrease as the inter layer coupling increases.

PACS numbers: 71.10.Fd, 74.20.Mn, 74.20.Rp

## I. INTRODUCTION

Understanding the competition between various magnetic orders and pairing symmetries is a major challenge in superconductivity now. The discovery of superconductivity in the  $\text{Na}_x\text{CoO}_2 \cdot y\text{H}_2\text{O}$  materials offer an appealing platform to investigate the interplay among pairing interactions, magnetic fluctuations, and electronic correlation<sup>1</sup>. Besides doped cuprates, cobaltates are another class of a layered 3d transition-metal oxide in which the superconductivity has been observed. The main difference between the two systems is that Co ions form a triangular lattice with magnetically frustrated geometry in contrast to the square lattice of the  $\text{CuO}_2$  plane. In doped cuprates, it has been well established that the  $\text{Cu}^{2+}$  moments are antiferromagnetically ordered in the  $\text{CuO}_2$  plane, and with a low level of carrier (hole or electron) doping, the antiferromagnetism is suppressed drastically, and the system becomes metallic, followed by the appearance of superconductivity where the  $d_{x^2-y^2}$  pairing symmetry dominates in the optimally doped region<sup>2-6</sup>. In general, the doping dependence of the pairing symmetry and the issue of quantum criticality must be considered under the premise of spatial homogeneity in the pairing potential. Results of some experiments suggest triplet pairing in cobaltates<sup>7,8</sup>, while some other measurements have resulted in contradicting conclusions which indicate singlet pairing<sup>9,10</sup>.

To investigate the superconducting mechanism of  $\text{Na}_x\text{CoO}_2 \cdot y\text{H}_2\text{O}$  system, the triangular lattice has been extensively studied theoretically<sup>11-20</sup>. In the Hubbard type model for this frustrated system, perturbation theory shows that  $d$ -wave and  $p$ -wave superconducting states are stable in hole doped region<sup>21</sup>, while the renormalization group approach suggests the  $d+id$ -wave pairing symmetry in the case with the antiferromagnetic exchange

interactions<sup>15</sup>. In the strong-coupling Hubbard model or in its strong coupling limits, the  $t$ - $J$  model, mean field results again support the  $d+id$ -wave superconductivity near the half-filling<sup>11-13</sup>, which has been confirmed by the variational Monte Carlo study<sup>22</sup>, while in the low density region where the Fermi surface is detached,  $f$ -wave pairing is proposed to be realized<sup>12</sup>. Then, the results obtained above are still actively debated because they are very sensitive to the approximation used, exact numerical results are highly desirable for they provide unbiased information and would serve as useful benchmarks for analytical approach. Moreover, understanding of the magnetic order and pair symmetries of frustrated system are still missing. For example, the situation of the pairing symmetry in  $\kappa$ -(ET)<sub>2</sub>X is complicated owing to the existence of frustration<sup>23</sup>. In a frustrated quantum antiferromagnet, the introduction of doping with mobile charge carriers may result in the appearance of unconventional superconductivity<sup>24</sup>. Bilayer triangular lattice is an idea platform to study the interplay between magnetic fluctuation and pairing correlation in frustrated system.

Again similar to the doped cuprates,  $\text{Na}_x\text{CoO}_2 \cdot y\text{H}_2\text{O}$  are layered materials, where the distance and couplings between the two  $\text{CoO}_2$  layers depend on the  $\text{H}_2\text{O}$  molecules inserted<sup>25-28</sup>, and the inter layer coupling term is also regarded as a key to understand the superconducting mechanism. Thus, in this paper, we study the magnetic and pairing correlation within the Hubbard model on a bilayer triangular lattice by using the determinant Quantum Monte Carlo simulations, which is a method that do not rely on uncontrolled approximations<sup>29-33</sup>. Numerical calculation reported here include results for a variety of band fillings, temperatures, pairing symmetries, and inter layer coupling terms. It is found that the system shows an antiferromagnetic correlation around the half filling, and the  $fn$ -wave pairing correlation dominates over other kinds of pairing symmetry in low doping region. As the electron filling decreases, both the ferromagnetic fluctuations and the  $f$ -wave pairing susceptibility

\*txma@bnu.edu.cn

ity are enhanced and tend to dominate. It is also shown that the magnetic correlation and pairing susceptibility decreases as the inter layer coupling increases. These results indicate that the competition of ferromagnetic and antiferromagnetic fluctuations in different filling region is crucial on the pairing behavior, which could be understood from the shape of the density of state (DOS) distribution in bilayer triangular lattice.

## II. MODEL

The sketch for the bilayer triangular lattice has been shown in Figs. 1 (a) and (b). As shown in Fig. 1(a), the model for each layer is set on a triangular lattice with hexagonal shape. There are  $2N$  sites on the diagonal, and the site number of this series of lattice is  $3N^2$ . This lattice setting reserves most geometric symmetries of the triangular lattice. Fig. 1(b) indicates the sketch for the interlayer hopping, and hence the total sites for such bilayer triangular lattice is  $2 \times 3N^2$ . The case of  $N = 4$  is shown here. The data points in the first Brillouin zone (BZ) include all the high symmetry points such as  $\Gamma$ ,  $M$ , and  $K$ , are shown in Fig. 1(c). For any atom, it has six nearest neighbor atoms in the same layer and three in the other layer, which could be described as

$$H = t \sum_{\langle i,j \rangle d\sigma} (c_{id\sigma}^\dagger c_{jd\sigma} + h.c.) + t' \sum_{\langle i,j \rangle \sigma} (c_{i1\sigma}^\dagger c_{j2\sigma} + h.c.) + U \sum_{id} n_{id\uparrow} n_{id\downarrow} - \mu \sum_{id\sigma} n_{id\sigma} \quad (1)$$

where  $c_{id\sigma}$  ( $c_{id\sigma}^\dagger$ ) annihilates (creates) electrons at the site  $R_i$  in the  $d$ -th layer ( $d = 1, 2$ ) with spin  $\sigma$  ( $\sigma = \uparrow, \downarrow$ ) and  $n_{id\sigma} = c_{id\sigma}^\dagger c_{id\sigma}$ . This system has intra layer nearest neighbor hopping  $t$  and inter layer hopping term  $t'$ , and these two layers have the same chemical potential  $\mu$ , as well as the electron-electron Coulomb interaction  $U$ . The system was simulated using determinant quantum Monte Carlo at finite temperature, and our numerical calculations were mainly performed on a  $2 \times 48$  ( $N=4$ ),  $2 \times 75$  ( $N=5$ ) and  $2 \times 108$  ( $N=6$ ) lattices with periodic boundary conditions.

It is generally believed that magnetic excitation might play a fundamental role in the superconducting mechanism of electronic correlated systems. To study the magnetic properties, we define the spin susceptibility in the  $z$  direction at zero frequency,

$$\chi(q) = \int_0^\beta d\tau \sum_{d,d'=1,2} \sum_{i,j} e^{iq \cdot (i_d - j_{d'})} \langle m_{id} \cdot m_{jd'} \rangle, \quad (2)$$

where  $m_{id}(\tau) = e^{H\tau} m_{id}(0) e^{-H\tau}$ ,  $m_{id} = c_{id\uparrow}^\dagger c_{id\uparrow} - c_{id\downarrow}^\dagger c_{id\downarrow}$ , and  $N_s$  represents the unit number of the lattice. To understand the superconductivity in  $\text{Na}_x\text{CoO}_2 \cdot y\text{H}_2\text{O}$  materials, the behavior of pairing is one of key issues. The property of pairing could be governed by the

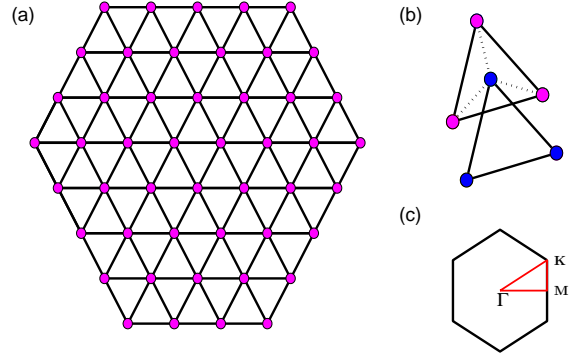


FIG. 1: (Color online) (a) Sketch of the triangular lattice, (b) bilayer triangular lattice structure and (c) the first Brillouin zone. The red line represent the high symmetry points including  $\Gamma$ ,  $M$  and  $K$  points.

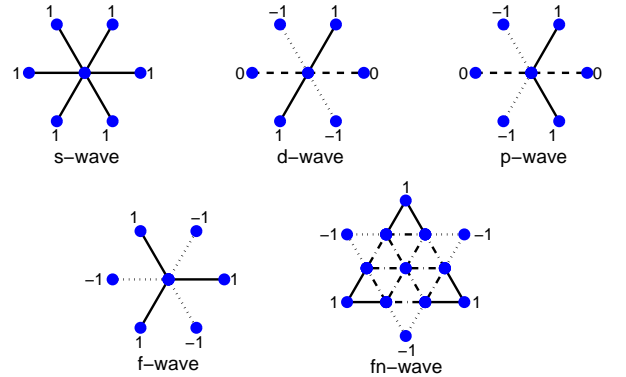


FIG. 2: (Color online) Site-dependent form factors for  $s$  wave,  $d$  wave,  $p$  wave,  $f$  wave, and  $fn$  wave pairing correlation functions in the triangular lattice.

pairing susceptibility at zero frequency, which is defined as

$$P_\alpha = \frac{1}{N_s} \sum_{i,j} \int_0^\beta d\tau \langle \Delta_\alpha^\dagger(i, \tau) \Delta_\alpha(j, 0) \rangle, \quad (3)$$

and

$$\begin{aligned} \Delta_\alpha(\tau) &= \frac{1}{\sqrt{N_s}} \sum_i \Delta_\alpha(i, \tau) \\ &= \frac{1}{\sqrt{N_s}} \sum_{i,l} f_\alpha(l) \langle c_{i\uparrow}(\tau) c_{i+l\downarrow}(\tau) \pm c_{i+l\uparrow}(\tau) c_{i\downarrow}(\tau) \rangle, \end{aligned} \quad (4)$$

where  $\alpha$  denotes the symmetry of the pairing function,  $i$  is the lattice site,  $l$  indicates the neighboring sites, and  $f_\alpha(l)$  is the site-dependent form factor of electron pairs. Considering the symmetry of the triangular lattice, possible form factors include the six types:  $f_s(l)$ ,  $f_{d_{xy}}(l)$ ,  $f_{d_{x^2-y^2}}(l)$ ,  $f_f(l)$ ,  $f_{p_x}(l)$ , and  $f_{p_y}(l)$ . The detail forms of these pairing symmetries have been discussed by T. Koetsune and M. Ogata in Ref.<sup>17</sup>. Following them, the possible form factors of the pairing correlation functions in the triangular lattice have been shown in Fig. 2.

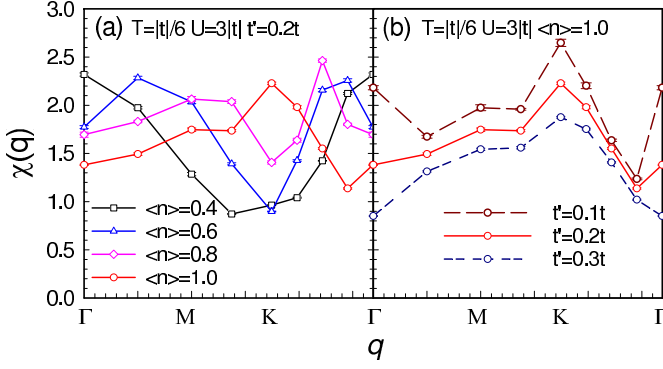


FIG. 3: (Color online) Spin susceptibility  $\chi(q)$  versus the momentum  $q$  (a) at various electron filling for  $U = 3|t|$ ,  $t' = 0.2t$ ,  $T = |t|/6$  and (b) at half filling for different  $t'$ . Data are shown along the path  $\Gamma \rightarrow M \rightarrow K \rightarrow \Gamma$  in the hexagonal BZ.

The former three are singlet pairing and the latter two are triplet case. As the triangular lattice is isotropic, the  $d_{xy}$ -wave and  $d_{x^2-y^2}$ -wave are degenerate, and the same goes for the  $p_x$ -wave and  $p_y$ -wave, here, we denote them as the  $d$ -wave and  $p$ -wave respectively<sup>17,18</sup>.

### III. RESULTS AND DISCUSSION

By using the determinant Quantum Monte Carlo method, one author of us and his collaborators have studied the magnetic correlation of the bilayer triangular lattice on the basis of single-band Hubbard model, in which the ferromagnetic fluctuations near the van Hove singularities were reported<sup>29</sup>, and the doped region is  $0.60 \sim 0.85$ , which corresponding to the electron filling  $0.40 \sim 0.15$  in current case. In Fig.3, we present the spin susceptibility  $\chi(q)$  in the electron filling region from  $< n > = 0.40$  to  $1.0$ , especially when the system is around the half filling with different inter layer coupling terms  $t'$ . Fig. 3 (a) shows  $\chi(q)$  versus the momentum  $q$  at  $< n > = 1.0$  (red line with circle),  $< n > = 0.8$  (dark line with square),  $< n > = 0.6$  (blue line with triangular) and  $< n > = 0.4$  (pink line with diamond) for  $U = 3|t|$ ,  $t' = 0.2t$  and  $T = |t|/6$ . At half filling, the peak of spin susceptibility is located at  $K$  point. When the system is doped away from the half filling, the peak of  $\chi(q)$  moves to the  $\Gamma$  point. Here,  $\chi(K)$  measures the antiferromagnetic correlation and  $\chi(\Gamma)$  measures the ferromagnetic fluctuations. Hence, the antiferromagnetic correlations dominate around the half filling region and ferromagnetic fluctuation dominates in the low electron fillings. Fig. 3 (b) shows the  $\chi(q)$  with different inter layer coupling terms  $t'$  at the half filling for  $U = 3.0|t|$  and  $T = |t|/6$ . One can see that the peak of the spin susceptibility  $\chi(q)$  is located at  $K$  point, while  $\chi(q)$  is suppressed as  $t'$  increases.

Such suppression, as well as the competition between ferromagnetic and antiferromagnetic correlation, could be understood from the property of the DOS in bilayer

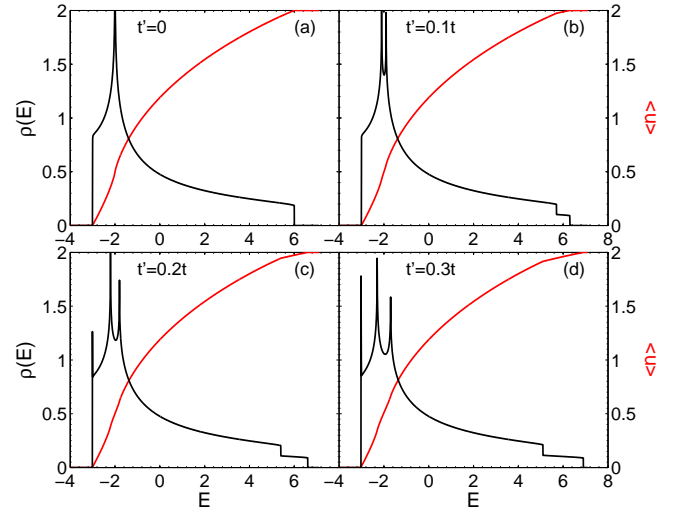


FIG. 4: (Color online) Dos and band fillings are functions of energy with (a)  $t' = 0$ , (b)  $t' = 0.1t$ , (c)  $t' = 0.2t$  and (d)  $t' = 0.3t$ , where the red lines represent fillings  $< n >$  and the black lines represent the DOS.

triangular lattice. The DOS and band fillings with different  $t'$  have been shown in Fig. 4 as function of energy. One can see that, for the single-layer triangular lattice ( $t' = 0$  in current case), its DOS in the non-interacting case has one van Hove singularity as the system is  $0.5$  doped away from the half filling. As the inter layer coupling term  $t'$  is introduced, the Van Hove singularity in the DOS tends to move further away from the half filling. According to the itinerant electron ferromagnetic theory, the ferromagnetic fluctuations tend to the higher DOS on the Fermi surface, so ferromagnetic correlation dominates in low electron filling region. As a result, the spin correlation at  $\Gamma$  point is suppressed as the inter layer coupling term increases at half filling.

Regarding the ferromagnetic correlation and the antiferromagnetic fluctuation shown in Fig.3 at different electron fillings, the competition between them indicates that pairing properties in such system may also be dependent on the electron fillings. Fig. 5 presents the temperature dependence of pairing susceptibility with different symmetries at (a)  $< n > = 0.4$ , (b)  $< n > = 0.6$ , (c)  $< n > = 0.8$  and (d)  $< n > = 1.0$  for  $U = 3|t|$  and  $t' = 0.2t$ . Basically, the behaviors of pairing susceptibility with all kinds of symmetry do not change qualitatively in the major part of the temperature region we studied. In the low electron filling region, as that shown in Fig. 5 (a) and (b), it is clear to see that the spin triplet  $f$ -wave,  $p$ -wave and the spin singlet  $d$ -wave pairing susceptibilities keep growing; especially, the  $f$  wave grows fastest. The  $fn$ -wave and  $s$ -wave pairing susceptibilities tend to saturate at  $< n > = 0.4$ . At  $< n > = 0.8$ , Fig.5 (c) shows the  $fn$  and  $f$ -wave pairing susceptibility contest the “race” closely in the whole temperature region. As the electron filling increases up to the half filling, as that shown in Fig. 5 (d), the  $fn$ -wave pairing suscep-

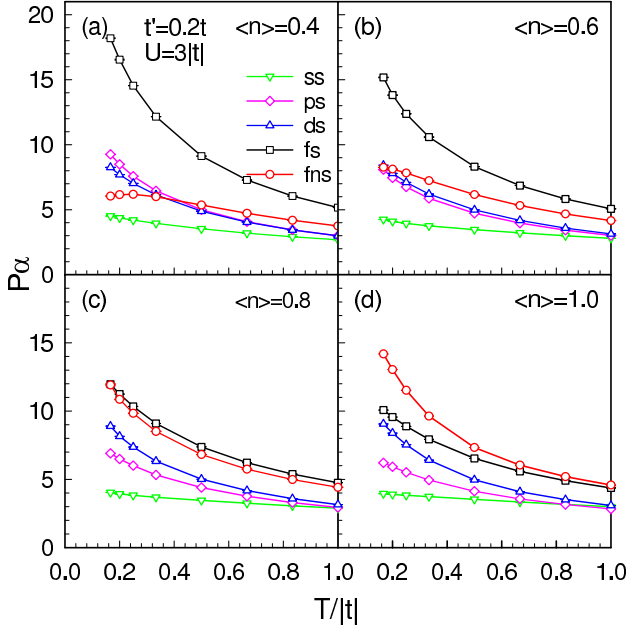


FIG. 5: (Color online) Pairing susceptibility for different pairing symmetries (ss:  $s$  wave, ps:  $p$  wave, ds:  $d$  wave, fs:  $f$  wave, fns:  $fn$  wave) versus the temperature  $T$  at  $U = 3|t|$  and  $t' = 0.2t$ . The sub-figures represent the situations of  $\langle n \rangle = 0.4$  (a),  $0.6$  (b),  $0.8$  (c), and  $1.0$  (d) respectively.

tibility tends to increase fastest, and the  $d$ -wave pairing susceptibility also has a potential to increase faster than the  $f$ -wave pairing susceptibility. However, due to the limitation of the numerical tool used here, we can not achieve arbitrarily low temperatures within the determinant Quantum Monte Carlo method, which experience the infamous fermion sign problem, and cases exponential growth in the variance of the computed results and hence an exponential growth in computer time as the lattice size is increased and the temperature is lowered. Basically, our numerical technology works well if the electron filling is not too close to the Van Hove singularity, and in the range of  $U/T \leq 36$ , the error bar could be controlled within one percent for a  $2 \times 48$  lattice.

Figs. 3 and 5 indicate that the competition of ferromagnetic and antiferromagnetic fluctuations in different filling region is crucial on the pairing behavior. Around half filling, the antiferromagnetic correlation dominates in the behavior of spin correlation, and the pairing susceptibility with  $fn$ -wave pairing symmetry is the most favorable. As the system is doped away from half filling, the ferromagnetic correlation tends to dominate over the antiferromagnetic correlation, and it is interesting to see that the  $f$ -wave pairing is the most favorable at the ferromagnetic fluctuation dominating region, which is consistent with previous work done by Kumar and Shastry<sup>12</sup>.

The temperature dependence of  $f$ -wave pairing susceptibility with different  $t'$  is presented in Fig. 6 (a) at  $\langle n \rangle = 0.40$  (solid lines) and  $\langle n \rangle = 1.0$  (dot lines). One can see that, the inter layer hopping has little in-

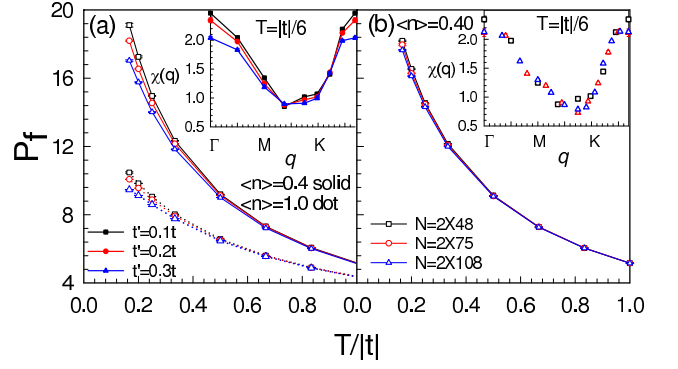


FIG. 6: (Color online) (a)  $f$ -wave pairing susceptibility at various inter layer coupling term  $t' = 0.1t$  (dark line with square),  $0.2t$  (red line with circle) and  $0.3t$  (blue line with triangular) versus the temperature  $T$  at  $\langle n \rangle = 0.40$  (solid lines) and  $\langle n \rangle = 1.0$  (dot lines) for  $U = 3|t|$ . Inset: The spin susceptibility at different  $t'$  for a  $2 \times 48$  lattice at  $T = |t|/6$ ,  $U = 3|t|$  and  $\langle n \rangle = 0.40$ . (b)  $f$ -wave pairing susceptibility for a  $2 \times 48$  lattice, a  $2 \times 75$  lattice and a  $2 \times 108$  lattice with  $t' = 0.2t$ ,  $U = 3|t|$  and  $\langle n \rangle = 0.4$ . Inset: The spin susceptibility for various lattices at  $T = |t|/6$ .

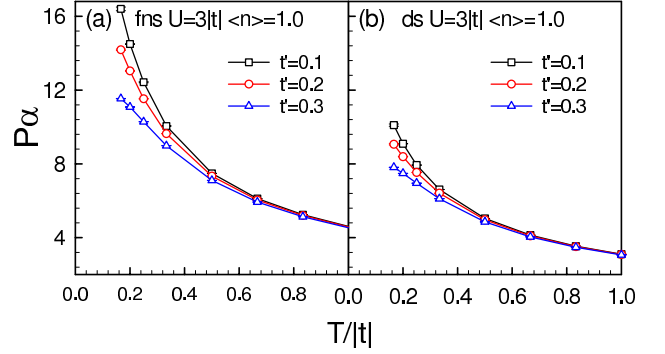


FIG. 7: (Color online) Pairing susceptibility at various inter layer coupling term  $t' = 0.1t$  (dark line with square),  $0.2t$  (red line with circle) and  $0.3t$  (blue line with triangular) versus the temperature  $T$  for  $U = 3|t|$  and  $n = 1.0$ . The sub-figures represent the situations of  $fn$ -wave (a) and  $d$ -wave respectively.

fluence on the  $f$ -wave pairing susceptibility, whatever for  $\langle n \rangle = 0.40$  or  $\langle n \rangle = 1.0$ . The  $t'$ -dependence of  $\chi(q)$  for  $\langle n \rangle = 0.4$  are also shown in the inset of Fig. 6 (a). The  $\chi(\Gamma)$  is suppressed very slightly as the  $t'$  increases, which is consistent with the behavior of the pairing correlation. In Fig.6 (b), the pairing susceptibility and spin susceptibility are shown on a  $2 \times 48$  lattice, a  $2 \times 75$  lattice and a  $2 \times 108$  lattice for  $t' = 0.2t$ ,  $U = 3|t|$  and  $\langle n \rangle = 0.4$ . Both the pairing susceptibility and spin susceptibility decrease slightly as the lattice size increases from  $2 \times 48$  to  $2 \times 75$ , and results for  $2 \times 75$  and  $2 \times 108$  are almost the same within the error bar. Hence we may argue here that the pairing and spin susceptibility is almost independent of the lattice size.

Fig. 5 shows that the  $fn$ - and  $f$ -wave pairings domi-



nate for  $\langle n \rangle > 0.8$  and  $\langle n \rangle < 0.8$ , respectively. The temperature dependence of  $f$ -wave pairing susceptibility and  $d$ -wave pairing susceptibility with different  $t'$  are shown in Fig. 7 (a) and (b) at  $\langle n \rangle = 1.00$ . At half filling, one can see that the pairing susceptibility is suppressed slightly by the increasing  $t'$ . This suppression is consistent with the behavior of spin susceptibility shown in Fig. 3 in which  $\chi(q)$  is also suppressed as the inter layer hopping term increases.

#### IV. CONCLUSION

To make a summary, we have studied the magnetic and pairing correlation of the single-band Hubbard model on a bilayer triangular lattice. We performed the determinant Quantum Monte Carlo simulations on the magnetic correlation and pairing susceptibility for a variety of electron fillings, temperatures and pairing symmetries. Around half filling, where the peak of the spin structure factor is located at  $K$  point, the  $f$ -wave pairing susceptibility dominates. As the electron filling decreases, the peak of spin correlation moves away from  $K$ , and finally locates at the  $\Gamma$  point<sup>29</sup>, which indicates the ferromagnetic fluc-

uation is stronger than the antiferromagnetic type when the electron filling is low enough. And the corresponding, the  $f$ -wave pairing susceptibility is enhanced and the  $f$ -wave pairing susceptibility is suppressed as the electron filling decreases, especially at low temperature. As a result, the  $f$ -wave pairing susceptibility dominates as the electron filling is lower than 0.8. Moreover, both the spin correlation and pairing susceptibility are suppressed by the increasing inter layer coupling  $t'$ . Note that our calculations only give reliable results at  $T > t/6$ . Therefore it is not conclusive whether the triplet  $f$ -wave really diverges or not as  $T \rightarrow 0$ . However, it would be important that there is a possibility of triplet superconductivity in the Hubbard model on a bilayer triangular lattice.

#### Acknowledgments

This work is supported by NSFC Grant. No. 11104014, Research Fund for the Doctoral Program of Higher Education of China 20110003120007, SRF for ROCS (SEM), and the Fundamental Research Funds for the Central Universities in China under 2011CBA00108.

- 
- <sup>1</sup> K. Takada, H. Sakurai, E. Takayama-Muromachi, F. Izumi, R. A. Dilanian, and T. Sasaki, Nature (London) **422**, 53 (2003).
  - <sup>2</sup> M. A. Kastner, R. J. Birgeneau, G. Shiran, and Y. Endoh, Rev. Mod. Phys. **70**, 897 (1998); Y. Tokura, H. Takagi, and S. Uchida, Nature (London) **337**, 345 (1989); H. Takagi, S. Uchida, and Y. Tokura, Phys. Rev. Lett. **62**, 1197 (1989).
  - <sup>3</sup> Patrick A. Lee, Naoto Nagaosa, and Xiao-Gang Wen Rev. Mod. Phys. **78**, 17 (2006)
  - <sup>4</sup> C.C. Tsuei and J. R. Kirtley, Rev. Mod. Phys. **72**, 969 (2000); C. Panagopoulos and T. Xiang, Phys. Rev. Lett. **81**, 2336 (1998).
  - <sup>5</sup> N.-C. Yeh, C. T. Chen, G. Hammerl, J. Mannhart, A. Schmehl, C.W. Schneider, R.R. Schulz, S. Tajima, K. Yoshida, D. Garrigus, M. Strasik, Phys. Rev. Lett. **87** 087003 (2001); A. Biswas, P. Fournier, M.M. Qazilbash, V.N. Smolyaninova, H. Balci, R.L. Greene, Phys. Rev. Lett. **88** 207004 (2002); C.C. Tsuei, J.R. Kirtley, G. Hammerl, J. Mannhart, H. Raffy, Z. Z. Li, Phys. Rev. Lett. **93** 187004 (2004).
  - <sup>6</sup> Shiping Feng, Phys. Rev. B **68**, 184501 (2003); Shiping Feng, Tianxing Ma, and Huaiming Guo, Physica C **436**, 14 (2006).
  - <sup>7</sup> W. Higemoto, K. Ohishi, A. Koda, S. R. Saha, R. Kadono, K. Ishida, K. Takada, H. Sakurai, E. Takayama-Muromachi, and T. Sasaki, Phys. Rev. B **70**, 134508 (2004).
  - <sup>8</sup> M. M. Maška, M. Mierzejewski, B. Andrzejewski, M. L. Foo, R. J. Cava, and T. Klimczuk, Phys. Rev. B **70**, 144516 (2004).
  - <sup>9</sup> G. Q. Zheng, K. Matano, D. P. Chen, and C. T. Lin, Phys. Rev. B **73**, 180503(R) (2006).
  - <sup>10</sup> T. Fujimoto, G. Q. Zheng, Y. Kitaoka, R. L. Meng, J. Cmaidalka, and C. W. Chu, Phys. Rev. Lett. **92**, 047004 (2004).
  - <sup>11</sup> G. Baskaran, Phys. Rev. Lett. **91**, 097003 (2003).
  - <sup>12</sup> B. Kumar and B. S. Shastry, Phys. Rev. B **68**, 104508 (2003).
  - <sup>13</sup> Q. H. Wang, D. H. Lee, and P. A. Lee, Phys. Rev. B **69**, 092504 (2004).
  - <sup>14</sup> A. Tanaka and X. Hu, Phys. Rev. Lett. **91**, 257006 (2003).
  - <sup>15</sup> C. Honerkamp, Phys. Rev. B **68**, 104510 (2003).
  - <sup>16</sup> K. Kuroki, Y. Tanaka, and R. Arita, Phys. Rev. Lett. **93**, 077001 (2004).
  - <sup>17</sup> T. Koretsune and M. Ogata, Phys. Rev. B **72**, 134513(2005).
  - <sup>18</sup> S. Q. Su, Z. B. Huang, R. Fan, and H. Q. Lin, Phys. Rev. B **77**, 125114 (2008).
  - <sup>19</sup> K. Kuroki, Y. Tanaka, and R. Arita, Phys. Rev. B **71**, 024506 (2005).
  - <sup>20</sup> M. D. Johannes, I. I. Mazin, D. J. Singh, and D. A. Papaconstantopoulos, Phys. Rev. Lett. **93**, 097005 (2004).
  - <sup>21</sup> Y. Nisikawa and K. Yamada, J. Phys. Soc. Jpn. **71**, 2629 (2002); H. Ikeda, Y. Nisikawa, and K. Yamada, J. Phys. Soc. Jpn. **73**, 17 (2004).
  - <sup>22</sup> T. Watanabe, H. Yokoyama, Y. Tanaka, J. Inoue, and M. Ogata, J. Phys. Soc. Jpn. **73**, 3404 (2004).
  - <sup>23</sup> R. T. Clay, H. Li and S. Mazumdar, Phys. Rev. Lett. **101**, 166403 (2008); S. Dayal, R. T. Clay, and S. Mazumdar, Phys. Rev. B **85**, 165141 (2012).
  - <sup>24</sup> J. Y. Gan, Y. Chen, and F. C. Zhang, Phys. Rev. B **74**, 094515 (2006).
  - <sup>25</sup> J. W. Lynn, Q. Huang, C. M. Brown, V. L. Miller, M. L. Foo, R. E. Schaak, C. Y. Jones, E. A. Mackey, and R. J. Cava, Phys. Rev. B **68**, 214516 (2003).
  - <sup>26</sup> J. D. Jorgensen, M. Avdeev, D. G. Hinks, J. C. Burley,

- and S. Short, Phys. Rev. B **68**, 214517 (2003).
- <sup>27</sup> M. D. Johannes and D. J. Singh, Phys. Rev. B **70**, 014507 (2004).
- <sup>28</sup> R. J. Xiao, H. X. Yang, and J. Q. Li, Phys. Rev. B **73**, 092517 (2006).
- <sup>29</sup> F. M. Hu, S. Q. Su, T. Ma, and H. Q. Lin, Phys. Rev. B **80**, 014428(2009).
- <sup>30</sup> R. Blankenbecler, D. J. Scalapino, and R. L. Sugar, Phys. Rev. D **24**, 2278 (1981).
- <sup>31</sup> Tianxing Ma, F. M. Hu, Z. B. Huang, and H. Q. Lin, Appl. Phys. Lett. **97**, 112504 (2010).
- <sup>32</sup> Tianxing Ma, H. Q. Lin, J. P. Hu, Phys. Rev. Lett. **110**, 107002 (2013).
- <sup>33</sup> Tianxing Ma, F. M. Hu, Z. B. Huang, and H. Q. Lin, Horizons in World Physics. **276**, Chapter 8, Nova Science Publishers, Inc., (2011).